

# Polymeric Catalysts Synthesized by the Hydrothermal Metal Deposition in the Fischer-Tropsch Synthesis

Mariia E. Markova<sup>a</sup>, Alexandra V. Gavrilenko<sup>b</sup>, Antonina A. Stepacheva<sup>b,\*</sup>, Valentina G. Matveeva<sup>b</sup>, Alexander I. Sidorov<sup>b</sup>, Mikhail G. Sulman<sup>b</sup>, Esther M. Sulman<sup>b</sup>

<sup>a</sup>Tver State Technical University, A. Nikitin str., 22, Tver, 170026, Russia

<sup>b</sup>Tver State University, Zhelyabova str., 33, Tver, 170100, Russia  
[a.a.stepacheva@mail.ru](mailto:a.a.stepacheva@mail.ru)

The search of the novel stable and active catalysts for the Fischer-Tropsch synthesis aimed at the formation of gasoline-range hydrocarbons is one of the main directions for the production of liquid transportation fuels from the alternative feedstock. The stabilization of the active phase is one of the key challenges for the development of the catalysts of CO hydrogenation into liquid motor fuel. This problem can be solved by the choice of optimal support as well as the method of synthesis. The rigid polymeric matrices allow obtaining highly effective and stable metal-containing nanoparticles characterized by the high surface area and enhanced activity. A hydrothermal deposition is a promising way to produce catalysts with the high dispersion of the active phase avoiding the pore blockage by the metal-containing particles. The current work is devoted to the development of novel polymer-based mono- and bimetallic Co-, Ni-, and Ru-containing nanocatalysts for the liquid-phase Fischer-Tropsch synthesis. It was shown that 1 % Ru-HPS and 10 % Co-1 % Ru-HPS allow obtaining a high yield of gasoline-range C<sub>5</sub>-C<sub>9</sub> hydrocarbons (over 70 %) providing high CO conversion (up to 23 %). The chosen polymer-based systems showed high stability in the FTS process. The activity loss was found to be insignificant for both catalysts (3.2 % for 1 % Ru-HPS, and 8.2 % for 10 % Co-1 % Ru-HPS) after 20 h of the process.

## 1. Introduction

The risen requirement in liquid fuels and increasing crude oil prices as well as environmental problems lead to the interest in shifting from fossil to renewable and waste feedstock as energy sources. Gasification of agricultural and domestic wastes or biomass results in the formation of gaseous mixture mainly consisting of carbon monoxide and hydrogen (Van Steen and Clayes, 2008). These gases are the most prospective feedstock for the production of fuels and valuable chemicals. A complex of the reactions between the carbon monoxide and hydrogen resulting in the formation of different compounds (alkanes, paraffin, olefins, oxygenates) is collectively called Fischer-Tropsch synthesis (FTS) (Zamani et al., 2015). Nowadays, FTS is the most intensely studied process. The researcher's interest is devoted to the development of novel techniques, catalysts, and equipment for the carbon monoxide hydrogenation in order to obtain high yields of the target products (Reactor et al., 2015). The molecular-weight-distribution of the FTS products depends on the reactor type, process conditions and the nature and structure of the catalyst (Li and Jens, 2014).

Nowadays, the interest of the researchers is focused on the development of novel highly effective and stable catalysts for FTS. Transition metals and their compounds such as nitrides, oxides, and carbides are the most active for the CO hydrogenation process. The highest catalytic activity can be observed while using Ru, Ni, Co, and Fe (Perego et al., 2009). The main problem of FTS catalysts is the active metal stabilization in order to prevent the aggregation and leaching of the active phase (Zhao et al., 2018). It is known that for the FTS catalysts, weak interaction between the support and active metal is one of the key factors (Oh et al., 2009). Nowadays, nano-scale mesoporous materials such as beta zeolites (Li et al., 2018), activated carbon (Zhao et al., 2018),  $\alpha$ -alumina (Rytter et al., 2019), titania (Kliwer et al., 2019) and graphene nanosheets (Taghavi et al., 2019) are widely used for the FTS. Moreover, there are some works devoted to the application of alumina coated with ZSM zeolite film (Zhu and Bollas, 2018) and metal-organic frameworks (MOF) (Isaeva et al., 2019)

as support for Co and Fe catalysts. Besides the support choice, the methods of metal deposition are also of great interest. Such novel approaches as aerosol synthesis (Martinez Arias and Weber, 2019), ultrasound deposition (Abbas et al., 2019), and pyrolysis (Zhao et al., 2018) were applied in order to stabilize the active phase on the supports.

As can be seen, the materials used as catalyst support for FTS have generally inorganic nature and, thus, can strongly affect the electron structure and composition of the active metal. Moreover, the inorganic materials have limited surface area and non-regular pore structure that can be critical for the product distribution of FTS. Rigid polymeric frameworks characterized by the high surface area and well-structured pores can be a promising alternative for the FTS catalyst supports. However, there is practically no information about the application of the polymer-based catalysts in CO hydrogenation. Thus, the current work is aimed at the study of the catalytic behavior of polymeric catalysts in FTS for the production of gasoline-range hydrocarbons.

## 2. Experimental

In the current work, the use of hypercrosslinked polystyrene (HPS) as an FTS catalyst support was proposed. This material due to its high surface area and rigid structure allows metal stabilization with high dispersion and, moreover, prevent the aggregation and leaching of the active phase (Stepacheva et al., 2016). Besides, such catalysts are stable to deactivation (Sidorov et al., 2017). However, HPS is considered to be microporous material. Hydrothermal synthesis of the catalysts applied in the current work allows changing the HPS porosity forming the pores with the mean diameter 20-50 nm, as it was shown recently (Stepacheva et al., 2018).

### 2.1 Materials

For the synthesis of the catalysts the following materials were used: cobalt (II) nitrate ( $\text{Co}(\text{NO}_3)_2 \cdot 6\text{H}_2\text{O}$ , C.P., Reachim, Russia), nickel nitrate ( $\text{Ni}(\text{NO}_3)_2 \cdot 6\text{H}_2\text{O}$ , C.P., Reachim, Russia), ruthenium hydroxohloride ( $\text{RuOHCl}_2$ , Aurat, Russia), sodium bicarbonate ( $\text{NaHCO}_3$ , C.P., Reachim, Russia), hypercrosslinked polystyrene (HPS MN-270, Purolight Inc., UK), distilled water.

In the catalyst testing experiments n-dodecane ( $\text{C}_{10}\text{H}_{22}$ , C.P., Reachim, Russia) and a gaseous mixture consisting of 20 vol. % of carbon monoxide (99.9 %, AGA, Russia) and 80 vol. % of hydrogen (99.9 %, AGA, Russia) was used.

### 2.2 Catalyst preparation

The catalysts were synthesized in stainless steel high-pressure reactor Parr-4307 (Parr Instrument, USA) according to the following procedure (Stepacheva et al., 2018): 1 g of HPS pre-treated with acetone, calculated amount of metal precursor, 0.1 g of sodium bicarbonate, and 15 mL of distilled water were placed into the reactor. The reactor was sealed and purged with nitrogen to remove the oxygen. The nitrogen pressure was set at 6.0 MPa. Then, the reactor was heated up to 200 °C and maintained for 15 minutes. After the reaction, the mixture was cooled to room temperature, filtered and washed with distilled water to remove anions. The following catalysts were obtained: 10 % Co-HPS, 1 % Ru-HPS, 10 % Co-1 % Ru-HPS, 10 % Ni-1 % Ru-HPS. The catalysts were preliminarily reduced in hydrogen flow at 300 °C for 4 h before the experiments. The catalyst characterization was performed by the low-temperature nitrogen physisorption, X-Ray photoelectron spectroscopy, and transmission electron microscopy.

### 2.3 Catalyst testing in FTS

The resulted catalysts were tested in the liquid-phase Fischer-Tropsch synthesis in a steel reactor PARR-4307 (Parr Instrument, USA) using n-dodecane as a solvent. A mixture of CO and H<sub>2</sub> in a volumetric ratio of 1:4 was used as synthesis gas. The high hydrogen content in the gas mixture is due to the need for additional hydrogenation of olefins and oxygen-containing compounds formed in the presence of cobalt- and iron-containing catalyst (Tomasek et al., 2018). The process temperature was 200 °C, the total pressure in the reactor was 2.0 MPa, the catalyst mass was 0.1 g, the solvent volume was 30 mL (Marques and Guirardello, 2018). The experiments were performed in a laboratory set-up shown in Figure 1: 1-4 – tanks with gases; 5 – gas distribution board; 6 – tank for synthesis-gas; 7- high-pressure reactor; 8 – return pressure valve; 9- gas chromatograph; 10 – flow-meter.

The liquid phase was analyzed by GCMS using GC-2010 gas chromatograph and GCMS-QP2010S mass spectrometer (SHIMADZU, Japan). The liquid phase analysis was carried out under the following conditions: the initial temperature of the column 150 °C was maintained for 6 min, then the temperature was raised up to 250 °C at a heating rate of 15 °C/min; injector temperature 280 °C; carrier gas-helium; pressure He 253.5 kPa; total flow He 81.5 mL/min; linear flow rate He 20.8 cm<sup>3</sup>/s; column HP-1MS: L = 30 m; d = 0.25 mm; film thickness 50 μm; ion source temperature 260 °C; interface temperature 280 °C; scanning mode from 10 to 800 m/z; scanning speed 625; electron impact ionization.

Analysis of the gas phase was carried out by a chromatographic method using gas chromatograph "Crystallux 4000M", equipped with a flame ionization detector and katharometer. To separate the components of the gas mixture, a 2.5 m long and 3.0 mm diameter Packed column filled with granules of polymer adsorbent MN270 (Purolight Inc., UK) with a fraction of 125-250  $\mu\text{m}$  was used. The gas phase analysis was carried out under the following conditions: initial temperature of the column 40  $^{\circ}\text{C}$ , maintained for 4 min, then, the temperature was raised up to 250  $^{\circ}\text{C}$  at a heating rate of 15  $^{\circ}\text{C}/\text{min}$ ; temperature of the evaporator and the detector 260  $^{\circ}\text{C}$ ; carrier gas – helium; total flow He 30.0 mL/min.

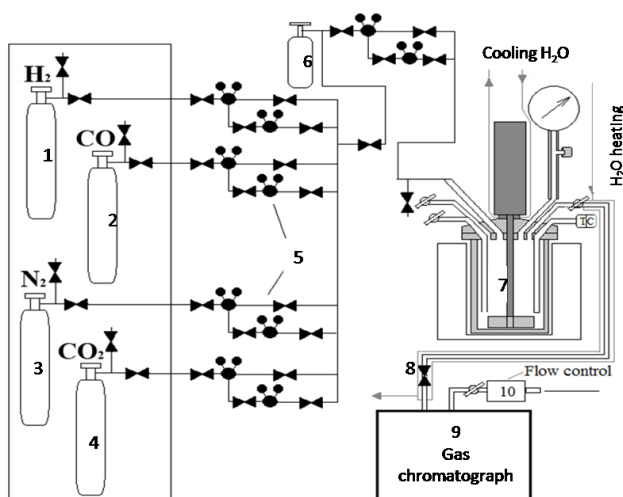


Figure 1: Experimental setup for liquid-phase FTS.

### 3. Results and discussion

First, monometallic catalysts were tested in the liquid-phase FTS. Analysis of CO conversion during the process showed that the use of the polymer-based catalysts provides significantly high reaction rates (5.8, 6.3, and 6.7  $\text{mmol}\cdot\text{g}_{\text{cat}}^{-1}\cdot\text{h}^{-1}$  for 10 % Co-HPS, 1 % Ru-HPS, and 10 % Ni-HPS respectively) in comparison with the literature data for liquid-phase process (Davis et al., 2002). The CO conversion degrees for all studied catalysts were found to be close to those for the classical gas-phase FTS (21.2, 21.9, and 22.3 % for 10 % Co-HPS, 1 % Ru-HPS, and 10 % Ni-HPS respectively) (Davis et al., 2002). Such high activity of the catalysts can be explained by the high specific surface area and higher accessibility of the catalyst active sites.

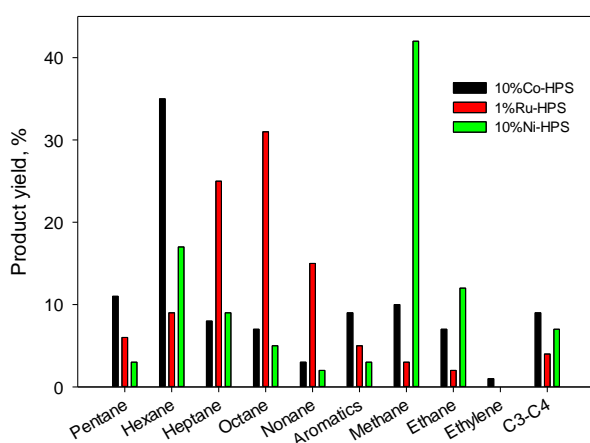


Figure 2: FTS product yields over monometallic polymer-based catalysts.

The analysis of the reaction products (Figure 2) showed that while using 10 % Ni-HPS catalyst, high amount of methane (over 40 %) is formed. However, because of the high adsorption ability of the support and the presence of large mesopores (Table 1), the formation of higher hydrocarbons ( $\text{C}_2\text{-C}_6$ ) was also observed (Dutta et al.,

2004). For Co-containing catalyst, a high yield of the linear C<sub>5</sub>-C<sub>9</sub> hydrocarbons (in total 73 %) was obtained. Meanwhile, the formation of light gases (in particular, methane – up to 10 %) was observed. It is interesting to note the formation of ethylene over the 10 % Co-HPS due to the low hydrogenation activity of cobalt, while Ni- and Ru-containing catalysts provided the formation of saturated hydrocarbons (Zhang et al., 2014). The use of 1 % Ru-HPS sufficiently decreases the formation of gaseous hydrocarbons (up to 9 %). While using a ruthenium catalyst, mainly C<sub>6</sub>-C<sub>9</sub> hydrocarbons (over 70 %) were obtained. In this case, octane was found to be the main reaction product.

In order to evaluate the influence of the Co and Ni addition to the ruthenium catalyst, the FTS was performed using bimetallic 10 % Co-1 % Ru-HPS and 10 % Ni-1 % Ru-HPS. The addition of iron subgroup metals to the ruthenium catalyst increases the CO conversion degree (up to 23.1 % for 10 % Co-1 % Ru-HPS) and the process average rate (up to 7.2 mmol·g<sub>cat</sub><sup>-1</sup>·h<sup>-1</sup>). Also, bimetallic catalysts showed a decrease in the methane yield as well as the total yield of gaseous hydrocarbons (Figure 3). The lowest methane yield (2 %) and the highest yield of C<sub>6</sub>-C<sub>7</sub> hydrocarbons (57 %) were observed while using 10 % Co-1 % Ru-HPS catalyst.

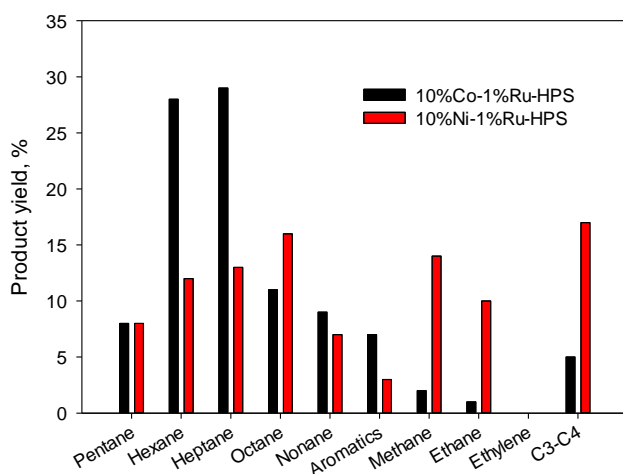


Figure 3: FTS product yields over bimetallic polymer-based catalysts.

Based on the catalyst testing results, 1 % Ru-HPS and 10 % Co-1%Ru-HPS were chosen as FTS catalysts providing the higher yield of the liquid gasoline-range hydrocarbons (over 70 %). The long-term stability of the chosen catalysts is shown in Figure 4.

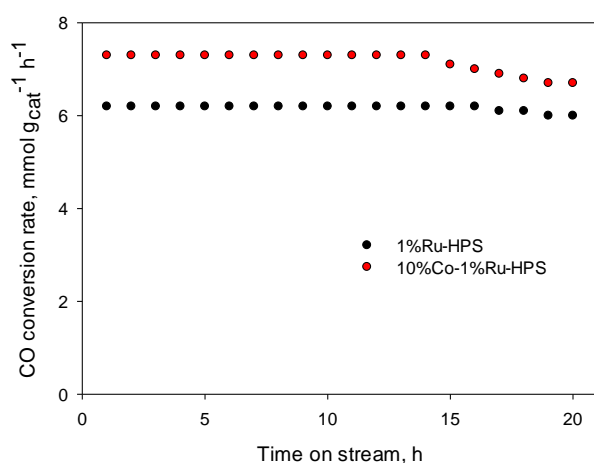


Figure 4: Catalyst long-time stability in liquid-phase FTS process.

As it is seen from Figure 4, the ruthenium-containing catalyst showed higher stability as compared with the bimetallic 10 % Co-1 % Ru-HPS. However, the decrease in the reaction rate was observed only after 15 h on time in the stream. Besides, the activity loss was found to be insignificant for both catalysts (3.2 % for 1 % Ru-

HPS, and 8.2 % for 10 % Co-1 % Ru-HPS) after 20 h of the process. The higher activity loss for the bimetallic catalyst can be connected to the slight surface carbonization as it was confirmed by XPS analysis (Tomashek et al., 2018).

In order to study the changes taking place during the catalyst synthesis and application, the physics-chemical analysis was performed. It was noted that the synthesized catalysts had a mesoporous structure with a high specific surface area and fine distribution of the active phase (Table 1). It is well known, that the catalysts characterized by the pore size 4-50 nm are the most optimal for FTS (Okabe et al., 2004). Thus, the hydrothermal method can be successfully applied for the preparation of FTS catalysts. The use of the catalysts slightly decreases the surface area due to the surface carbonization (up to 15 %) and leads to insignificant aggregation of the active phase, however, its composition does not change (Biesinger et al., 2011).

*Table 1: Catalyst characterization results*

Sample	Surface area, m <sup>2</sup> /g	Mean pore diameter, nm	Particle diameter, nm	Surface metal concentration, at. %	Metal compound	Surface carbonization degree, %
HPS	1400	4.5	-	-	-	-
1 % Ru-HPS initial	1100	4.5, 20-50	3.5	0.4	RuO <sub>2</sub>	-
1 % Ru -HPS after 20 h in stream	1050	4.5, 20-50	3.6	0.45	RuO <sub>2</sub>	5
10 % Co-1 % Ru-HPS initial	1000	4.5, 20-50	5.0	2.8, 0.3	Co <sub>3</sub> O <sub>4</sub> , RuO <sub>2</sub>	-
10 % Co-1 % Ru-HPS after 20 h in stream	900	4.5, 20-50	5.1	2.7, 0.35	Co <sub>3</sub> O <sub>4</sub> , RuO <sub>2</sub>	15

#### 4. Conclusions

In this paper, the performance of mono- and bimetallic catalysts synthesized by the hydrothermal deposition was studied in the liquid-phase FTS. 1 % Ru-HPS and 10 % Co-1 % Ru-HPS were found to be the most effective catalysts allowing obtaining a high yield (up to 73 %) of gasoline-range C<sub>5</sub>-C<sub>9</sub> hydrocarbons. Ru-catalyst showed higher selectivity towards the formation of C<sub>8</sub>-C<sub>9</sub> hydrocarbons (up to 50 %), while the shift in the selectivity towards C<sub>6</sub>-C<sub>7</sub> hydrocarbons (up to 57 %) for Co-Ru bimetallic catalysts was observed. The chosen polymer-based systems showed high stability in the FTS process. The decrease in the activity was found to be 3-8 % after 20 h in time on stream. The catalyst analysis showed that the synthesized catalysts had a mesoporous structure with a high specific surface area (over 1000 m<sup>2</sup>/g) and fine distribution of the active phase.

Thus, it was shown that the polymer-based catalysts can be a promising alternative for the classical FTS catalysts in terms of activity, stability, and selectivity. The rigid polymer structure coupling with the hydrothermal deposition allows fine stabilization of the active phase preventing its aggregation, leaching, and fast carbonization. This study can be a platform for the future works on the polymer's application in CO hydrogenation processes. The further studies can be focused on the optimization of the catalyst composition, choosing the catalyst synthesis conditions as well as the optimization of the FTS reaction conditions.

#### Acknowledgments

The authors thank the Ministry of Science and Higher Education of the Russian Federation and the Russian Foundation for Basic Research (grant 17-08-00609, 18-29-06004, 17-08-00659).

#### References

- Abbas M., Xue Y., Zhang J., Chen J., 2019, Ultrasound induced morphology-controlled synthesis of Au nanoparticles decorated on Fe<sub>2</sub>O<sub>3</sub>/ZrO<sub>2</sub> catalyst and their catalytic performance in Fischer-Tropsch synthesis, *Fuel Processing Technology*, 187, 63-72.
- Biesinger M.C., Payne B.P., Grosvenor A.P., Lau L.W.M., Gerson A.R., Smart R.St.C., 2011, Resolving surface chemical states in XPS analysis of first-row transition metals, oxides, and hydroxides: Cr, Mn, Fe, Co and Ni, *Applied Surface Science*, 257, 2717-2730.
- Davis B.H., 2002, Overview of reactors for liquid phase Fischer–Tropsch synthesis, *Catalysis Today*, 71 (3–4), 249–300.
- Dutta P., Manivannan A., Seehra M.S., Adekknattu P.M., Guin J.A., 2004, Determination of the electronic state and concentration of nickel in NiSAPO catalysts by magnetic measurements, *Catalysis Letters*, 94, 181-185.

- Isaeva V.I., Eliseev O.L., Kazantsev R.V., Chernyshev V.V., Tarasov A.L., Davydov P.E., Lapidus A.L., Kustov L.M., 2019, Effect of the support morphology on the performance of Co nanoparticles deposited on metal-organic framework MIL-53(Al) in Fischer–Tropsch synthesis, *Polyhedron*, 157, 389–395.
- Kliwer C.E., Soled S.L., Kiss G., 2019, Morphological transformations during Fischer-Tropsch synthesis on a titania-supported cobalt catalyst, *Catalysis Today*, 323, 233–256.
- Li B., Jens K.J., 2014, Low-Temperature and Low-Pressure Methanol Synthesis in the Liquid Phase Catalyzed by Copper Alkoxide Systems, *Industrial and Engineering Chemistry Researches*, 53 (5), 1735–1740.
- Li H., Hou B., Wang J., Qin C., Zhong M., Huang X., Jia L., Li D., 2018, Direct conversion of syngas to isoparaffins over hierarchical beta zeolite supported cobalt catalyst for Fischer-Tropsch synthesis, *Molecular Catalysis*, 459, 106–112.
- Marques F.H., Guirardello R., 2018, Thermodynamic analysis for Fischer-Tropsch synthesis using biomass, *Chemical Engineering Transactions*, 65, 397–402.
- Martinez Arias A., Weber A.P., 2019, Aerosol synthesis of porous SiO<sub>2</sub>-cobalt-catalyst with tailored pores and tunable metal particle size for Fischer-Tropsch synthesis (FTS), *Journal of Aerosol Science*, 131, 1–12.
- Oh J.H., Bae J.W., Park S.J., Khanna P.K., Jun K.W., 2009, Slurry-Phase Fischer-Tropsch Synthesis Using Co/ $\gamma$ -Al<sub>2</sub>O<sub>3</sub>, Co/SiO<sub>2</sub> and Co/TiO<sub>2</sub>: Effect of Support on Catalyst Aggregation, *Catalysis Letters*, 130, 403–409.
- Okabe K., Li X.H., Wei M.D., Arakawa H., 2004, Fischer-Tropsch synthesis over Co-SiO<sub>2</sub> catalysts prepared by the sol-gel method, *Catalysis Today*, 89, 431–438.
- Perego C., Bortolo R., Zennaro R., 2009, Gas to Liquids Technologies For Natural Gas Reserves Valorization: The Eni Experience, *Catalysis Today*, 142, 9–16.
- Reactor T., Abatzoglou N., Legras B., 2015, Nano-Iron Carbide-Catalyzed Fischer-Tropsch Synthesis of Green Fuel: Surface Reaction Kinetics controlled Regimes in a 3- $\phi$  Slurry-Continuous Stirred, *International Journal of Environmental Pollution and Remediation*, 3, 9–15.
- Rytter E., Borg Ø., Enger B.C., Holmen A., 2019,  $\alpha$ -alumina as a catalyst support in Co Fischer-Tropsch synthesis and the effect of added water; encompassing transient effects, *Journal of Catalysis*, 373, 13–24.
- Sidorov A., Tkachenko O., Sulman E., Doluda V., Stepacheva A., 2017, X-Ray Absorption Spectroscopy study of ZnO-CuO-HPS catalyst, *Chemical Engineering Transactions*, 61, 607–612.
- Stepacheva A.A., Markova M.E., Bykov A.V., Sidorov A.I., Sulman M.G., Matveeva V.G., Sulman E.M., 2018, Ni Catalyst Synthesized by Hydrothermal Deposition on the Polymeric Matrix in Supercritical Deoxygenation of Fatty Acids, *Reaction Kinetics, Mechanisms and Catalysis*, 125, 213–226.
- Stepacheva, A.A., Matveeva, V.G., Sulman, E.M., Sapunov, V.N., 2016, Fatty acid hydrotreatment using hypercrosslinked polystyrene-supported Pd catalysts to produce biofuels, *Chemical Engineering Transactions*, 52, 625–630.
- Taghavi S., Tavasoli A., Asghari A., Signoretto M., 2019, Loading and promoter effects on the performance of nitrogen functionalized graphene nanosheets supported cobalt Fischer-Tropsch synthesis catalysts, *International Journal of Hydrogen Energy*, 44, 10604–10615.
- Tomasek S., Lonyi F., Valyon J., Wollmann A., Hancsok J., 2018, Fuel production from Fischer-Tropsch paraffin mixtures, *Chemical Engineering Transactions*, 70, 667–672.
- Van Steen E., Claeys M., 2008, Fischer-Tropsch Catalysts for the Biomass-to-Liquid Process, *Chemical Engineering and Technology*, 31 (5), 655–666.
- Zamani Y., Zamaniyan A., Bahadoran F., Shojaei M., 2015, Effect of Calcium Promoters on Nanostructured Iron Catalyst for Fischer-Tropsch Synthesis, *Journal of Petroleum Science and Technology*, 5 (1), 21–27.
- Zhang S.T., Yan H., Wei M., Evans D.G., Duan X., 2014, Hydrogenation mechanism of carbon dioxide and carbon monoxide on Ru (0001) surface: a density functional theory study, *RSC Advances*, 4, 30241–30249.
- Zhao X., Lu S., Wang L., Li L., Wang G., Zhang Y., Li J., 2018, Comparison of preparation methods of iron-based catalysts for enhancing Fischer-Tropsch synthesis performance, *Molecular Catalysis*, 449, 99–105.
- Zhu C., Bollas G.M., 2018, Gasoline selective Fischer-Tropsch synthesis in structured bifunctional catalysts, *Applied Catalysis B: Environmental*, 235, 92–102.